に対し電子顕微鏡観察用のグリッド標本を作成し、臨床診断プロファイルおよび、病理学的診断データ、電顕クロマチン各指標データの統合プロファイルを作成した。

2、心不全可塑性を示す新しい診断鑑別方法の確立

電顕クロマチン各指標データの計測に際しては、H23 年度に確立した独自クロマチン密度解析法により細胞核クロマチンの病態別サブタイプを同定するとともに、心不全可塑性判断指標となる新規パラメータを定義した。不全心筋細胞の細胞核のクロマチン構造の観察を行い、クロマチン構造による違いで 3 グループに分類した。構造指標と臨床診療データとの相関性に関する検討を行い、心不全可塑性に関する臨床判断が可能なクロマチンスコアを算出する。Acuracy の高い数値として cut off 値を求めることができた(論文作成中)。

求めたクロマチン指標により分類された各グループの細胞核クロマチン超微細構造を明らかにするために行った超高圧電子顕微鏡を用いた詳細な観察において、大阪大学超高電圧顕微鏡センター(100kv～1000kV 電圧の観察及び TEM トモグラフィーを用いた微細構造解析)の協力の下で、H23 年度に使用した検体と同一症例、同一心筋採取部位、同一標本(視野)の検体を用いることとした。超高圧電視顕微鏡による撮像を行い、再現性良くナノメートルレベルの解像度で細胞核内のクロマチン超微細構造を観察することができた。上記 3 グループに分類した核は、超高圧電子顕微鏡による観察で異なる構造形態を呈していた。透過型電子顕微鏡では観察し得ない、高解像度でかつ三次元構築されたクロマチン構造が観察し得た。

D. 考察

本研究の主幹をなす心筋細胞の細胞核クロマチン構造変化の計測指標が、Pilotデータ検証も終わり、母集団の拡大にも有意性を以て指標となり得ることが示唆された。

平成23年度より継続的に行っている、心機能改善の可塑性を表す指標の開発は、心不全診療にとって大きな診断マーカーとしての有用性が期待される。

本年度解析において作成したヒト臨床心不全のデータプロファイルより、心不全特異的に変化を示すエピゲノム分子およびその修飾、病理組織変化などがあることが示唆されことにより(論文作成中)、現在同定しつつあるこれら領域、蛋白の病態との相関性、機能解析を引き続き行い、生物学的意義も含めた統合的理解が得られるものと考えられる。

E. 結論

心不全可塑性を示す新しい、重症心不全病理画像解析技術の開発にあたって、超高圧電子顕微鏡による微細構造解析を行い、透過型電顕による撮像と相関していることが示唆された。心不全可塑性病理診断法の確立のため、病理組織所見と分子生物学的エピゲノム変化指標の検索を同時に同一サンプルで行うことが新しい診断分子の発見につながる。

今後も心筋細胞核クロマチン構造変化の臨床指標を独自に考案し、その指標の妥当性を臨床検査データとの相関を見つけることにより、基礎的病態解析を開始している。新規病理微細構造解析法における病態・病期を判断できることを目標とする。

F. 健康危険情報

現在まで有害の事象なし

G. 研究発表

1、論文発表

1) Kamimura D, Ohtani T, Sakata Y, Mano T, Takeda Y, Tamaki S, Omori Y, Tsukamoto Y, Furutani K, Komiyama Y, Yoshika M, Takahashi H, Matsuda T, Baba A, Umemura S, Miwa T, Komuro I, Yamamoto K.
Ca2+ entry mode of Na+/Ca2+ exchanger as a new therapeutic target for heart failure with preserved ejection fraction. Eur Heart J. 33:

1408-16. 2012.

2) Ohtani T, Mohammed SF, Yamamoto K, Dunlay SM, Weston SA, Sakata Y, Rodeheffer RJ, Roger VL, Redfield MM.
Diastolic stiffness as assessed by diastolic wall strain is associated with adverse remodelling and poor outcomes in heart failure with preserved ejection fraction. Eur Heart J. 33: 1742-9. 2012.

3) Minamiguchi H, Mizuno H, Masuda M, Sakata Y, Saito S, Nanto S, Sawa Y, Komuro I.
Catheter ablation of focal atrial tachycardia originating from a donor heart after bicaval orthotopic heart transplantation guided by a noncontact mapping system. Int Heart J. 53:146-8. 2012.

4) Omori Y, Ohtani T, Sakata Y, Mano T, Takeda Y, Tamaki S, Tsukamoto Y, Kamimura D, Aizawa Y, Miwa T, Komuro I, Soga T, Yamamoto K. L-Carnitine prevents the development of ventricular fibrosis and heart failure with preserved ejection fraction in hypertensive heart disease. J Hypertens. 30: 1834-44. 2012.

5) Takeda Y, Nakatani S, Kuratani T, Mizote I, Sakata Y, Torikai K, Shimamura K, Nanto S, Komuro I, Sawa Y.
Systolic anterior motion of the mitral valve and severe mitral regurgitation immediately after transcatheter aortic valve replacement J Echocardiogr. 10: 143-45. 2012.

7) Shudo Y, Nakatani S, Sakaguchi T, Miyagawa S, Yoshikawa Y, Takeda K, Saito S, Takeda Y, Sakata Y, Yamamoto K, Sawa Y.
Left ventricular mechanics following restrictive mitral annuloplasty for functional mitral regurgitation: Two-Dimensional speckle tracking echocardiographic study. Echoradiography.29:445-50.2012.

8) Kainuma S, Sakaguchi T, Saito S, Miyagawa S, Yoshikawa Y, Yamauchi T, Sakata Y, Takahashi A, Uehata T, Kuratani T, Sawa Y.
Implantation of a Jarvik 2000 left ventricular assist device as a bridge to eligibility for refractory heart failure with renal dysfunction. J Artif Organs. 15: 83-86. 2012.

9) Yoshida A, Mizote I, Sakata Y, Maeda T, Kanakura Y, Yamauchi-Takihara K, Komuro I.
Effect of vasodilators in patient with pulmonary hypertension associated with hemolytic anemia. Journal of Cardiology Cases. 6; e75-e77. 2012.

10) Ichibori Y, Nakatani D, Sakata Y, Tachibana K, Akasaka T, Saito S, Fukushima N, Sawa Y, Nanto S, Komuro I.
Cardiac Allograft Vasculopathy Progression Associated With Intraplaque Neovascularization. J Am Coll Cardiol, 61, e149. 2013.

(和文)

1) 大谷朋仁、坂田泰史
エプレレノンは値段の高いスピロノラクトンか
循環器内科 71(1):64-68, 2012.

2) 坂田泰史
左室駆出率を保った心不全症例における死亡様式 : I-Preserve 試験からの検討
FluidManagenmentRenaissance 2(1):75-76,2012.

3) 坂田泰史
慢性心不全の再入院予防の薬物治療
Therapeutic Research 33(1):38-44,2012.

4) 坂田泰史
強心薬 心臓 44(5):540-545,2012.

5) 坂田泰史 低K血症
FluidManagenmentRenaissance 2(2):34-40,2012.

6) 大森洋介・坂田泰史
心不全における心腎連関
呼吸と循環 60(7):719-722,2012.

7) 坂田泰史
肺高血圧における左室の変形は何を語っているのか
月刊心エコー 13(5):482-490,2012.

8) 坂田泰史
Nohria 分類と Forrester 分類
AnnualReview 循環器 125-129,2012. 中外医学社.

9) 坂田泰史
心不全の新しい分類を臨床にどのように活用す

るか
心臓血管画像 116-118,2012. 産業開発機構株式会社.

2、学会発表
なし

H. 知的財産権の出願・登録状況
(予定も含む)

1、特許取得
なし

2、実用新案登録
なし

3、その他
以上、特筆すべき事項なし

厚生労働科学研究費補助金(創薬基盤推進研究事業)

分担研究報告書

臨床心不全エピゲノム診断における組織可塑性指標となる新規サロゲートマーカーの開発と治療への応用に関する研究

研究分担者　山崎 悟　国立循環器病研究センター　室長

研究要旨

核蛋白ヒストンや DNA メチル化に代表されるエピゲノム分子修飾は、循環器病態においても重要な機序に関わると類推され、ゲノムワイドな解析が待たれる。そこで、超高速 DNA シーケンスによるヒストン修飾と RNA 発現、細胞核超微細構造の各解析と臨床指標との比較を検討するとともに、各分子修飾の動物病態モデルにおける評価を行う。さらに心不全のエピゲノム・遺伝子発現プロファイルを作成し、病態と関連する核内蛋白の新規スクリーニングを行い、同定した心不全可塑性サロゲートマーカーの臨床心不全への有用性を検討する。

A. 研究目的

病態進展と治療抵抗性を決める心筋可塑性を表す新規サロゲートマーカーが必要である。ヒト臨床検体をもとにしたゲノムワイドなエピゲノム解析を行うことにより、未だ実用化されていない、心不全可塑性の分子指標を開発する。

B. 研究方法

1、ヒト臨床心不全特殊生体試料を利用したエピゲノム解析

① Genome-wideなDNAメチル化およびヒストン修飾解析

超高速 DNA シーケンサーを用い、遺伝子転写活性化を示すヒストン修飾 histoneH3K4me3 および抑制性を示す指標として histoneH3K27me3、さらに転写複合体の結合部位探索のため RNA polymerase II、ほか有意な転写制御を鑑別可能な抗体を用いて、genome-wide にクロマチン免疫沈降 ChIP-sequence 解析を行う。

説明と同意書の取得の後に採取されたヒト臨床不全心筋組織試料、不全心筋組織、正常心筋組織をそれぞれ 2 検体で比較し、病態変化にともなう転写因子複合体やエピゲノム修飾のゲノム上の感受性領域を検討する。

② 超高速シークエンシングによるRNA発現解析と心不全関連遺伝子プロファイル作成

心臓移植ないし心補助循環治療を行った際に説明と同意書の取得の後に採取されたヒト臨床不全心筋組織試料を用いて RNA 発現解析を行い、心不全エピゲノムおよび遺伝子発現プロファイルの統合データプロファイルを作成する。

超高速シークエンシングによる RNA 発現解析と心不全関連遺伝子プロファイルとのデータを統合し比較し、Genome-wide な DNA メチル化解析、ヒストン修飾解析、超高速シーケンシングによる RNA 発現解析において

作成した心不全関連遺伝子プロファイルを作成する。

2、心不全可塑性を示す新しい診断鑑別方法の確立

心不全エピゲノムおよび遺伝子発現プロファイルの作成

Genome-wide な DNA メチル化解析、ヒストン修飾解析、超高速シーケンシングによるRNA 発現解析において作成した心不全関連遺伝子プロファイルから、心臓特異的機能変化を持つと考えられる遺伝子リストを作成し、心不全可塑性に関するエピゲノム診断に用いる分子マーカーを同定する。

（倫理面への配慮）

患者情報の解析に関しては施設の倫理委員会の承認を得た上、臨床研究倫理指針を遵守し慎重におこなう。その上で患者とは個別に、医師が書面に示した計画書を明示し、十分説明をしたうえで承諾を得たもののみを本研究に使用する。特に以下の点に留意する。

1）試料提供者の個人識別情報を含む情報の保護：診療情報を含めた個人情報と検体とは徹底した匿名化を行い、遺伝情報と個人情報の連結は個人識別情報管理者のみが可能となるように個人識別情報管理者をおいて情報を管理する。

2）試料提供者に対する予想される危険や不利益およびそれらが生じた場合の措置：心筋生検試料採取は通常の診療の際に医学的必要に応じて行われたもののうち、診療に用いない残余検体を利用することとし、危険や不利益はないと考える。誤って遺伝情報が外部に漏洩した場合、就職・結婚・保険への加入等に関して不利益をこうむる可能性が考えられるため、これを防ぐために、個人識別情報管理者を置き、同管理者は試料の匿名化を行うとともに個人情報を厳重に管理・保管し、試料提供者のプライバシーを保護する。

3）試料提供者から採取した生体材料の取り扱いについて：提供された試料は、個人識別情報管理者が連結匿名化し、匿名化ラベルのみ貼って保存する。これらの試料は、生体試料の包括利用同意を得ており、本研究だけでなく、将来倫理委員会で承認された他の自主臨床研究についても用いることが可能である。したがって検査済みの試料は、適宜連結可能匿名化番号を含む検体等を完全に削除した上で廃棄するが、使用可能な残余検体は匿名化されたまま施錠された保管場所で保管される。また、特に研究成果として得られた情報の管理には、外部に漏洩しないように対策を行う。

動物実験においても愛護上の問題点を考慮の上、施設の審査結果を本研究について得た。この倫理規定にのっとり動物愛護上の配慮を十分行って実験をおこなう。

C. 研究結果

1、ヒト臨床心不全特殊生体試料を利用したエピゲノム解析

① Genome-wideなDNAメチル化およびヒストン修飾解析

ヒト臨床不全心筋組織試料、不全心筋組織、正常心筋組織をそれぞれ 2 検体ずつで比較し、病態変化にともなう転写因子複合体やエピゲノム修飾のゲノム上の感受性領域を検討するため、超高速 DNA シーケンサーを用い、遺伝子転写活性化を示すヒストン修飾 histoneH3K4me3 および抑制性を示す指標として histoneH3K27me3、さらに転写複合体の結合部位探索のため RNA polymerase II、ほか有意な転写制御を鑑別可能な抗体を用いて、genome-wide にクロマチン免疫沈降(ChIP)-sequence 解析を行った。RNA-seq についても現在多検体のシーケンス解析を行っている過程にある。

② 超高速シークエンシングによるRNA発現解析と心不全関連遺伝子プロファイル作成

心臓移植ないし心補助循環治療を行った際に説明と同意書の取得の後に採取されたヒト臨床不全心筋組織試料を用いて RNA 発現解析を行い、心不全エピゲノムおよび遺伝子発現プロファイルの統合データプロファイルを作成する。

超高速シークエンシングによる RNA 発現解析と心不全関連遺伝子プロファイルとのデータを統合し比較し、Genome-wide な DNA メチル化解析、ヒストン修飾解析、超高速シーケンシングによる RNA 発現解析において作成した心不全関連遺伝子プロファイルを作成する。

2、心不全可塑性を示す新しい診断鑑別方法の確立

心不全エピゲノムおよび遺伝子発現プロファイルの作成

Genome-wide な DNA メチル化解析、ヒストン修飾解析、超高速シーケンシングによる RNA 発現解析において作成した心不全関連遺伝子プロファイルから、心臓特異的機能変化を持つと考えられる遺伝子リストを作成し、心不全可塑性に関するエピゲノム診断に用いる分子マーカーを同定する。

次世代シーケンサーのデータ解析パイプラインを構築した LINUX サーバー(OS: CentOS 6.0, 64bit, Intel core i7-2600 4core)とオープンソースを中心とした特殊ソフトウェアの導入により、データのクオリティチェック、リファレンスマッピング、アプリケーションごとの解析を行うべく、スクリプト作業を行い、膨大なデータ解析に対応できる情報解析環境を本研究システムに構築し得た。最終的にはエピゲノム解析データと同一ゲノム Viewer 上で比較可能なように、データプロファイルを作るための情報解析スクリプトを作成中である。

D. 考察

心不全特異的に変化を示すエピゲノム分子およびその修飾、病理組織変化などがあることが示唆されている。心臓生体試料のクロマチン免疫沈降法の独自開発とその解析データプロファイルの構築することが重要である。ヒト臨床検体を用いた病態に準拠した組織エピゲノム解析は未だ少なく、本研究によって構築される心臓データプロファイルは、様々な研究に利用することが可能であり、広い応用のためにも完成を急ぐ必要がある。

E. 結論

心不全エピゲノムおよび遺伝子発現プロファイルおよびエピゲノムプロファイルから心不全病態に特異的なエピゲノム変化領域および分子修飾、DNA 結合蛋白の同定を行った。

ヒト臨床心不全特殊生体試料を利用したエピゲノム解析を行い、Genome-wide な DNA メチル化およびヒストン修飾解析、超高速シークエンシングによる RNA 発現解析と心不全関連遺伝子プロファイルの作成を行った。修飾分子、病態サンプル別にさらにプロファイルの比較サンプルを現在もなお増やしている段階にある。

F. 健康危険情報

現在まで有害の事象なし

G. 研究発表

1、.論文発表

(英文原著)

1) Yoshida A, Asanuma H, Sasaki H, Sanada S, Yamazaki S, Asano Y, Shinozaki Y, Mori H, Shimouchi A, Sano M, Asakura M, Minamino T, Takashima S, Sugimachi M, Mochizuki N, Kitakaze M.
H(2) mediates cardioprotection via involvements of K(ATP) channels and permeability transition pores of mitochondria in dogs. Cardiovasc Drugs Ther. 26(3):217-26. 2012.

2) Takahashi A, Asakura M, Ito S, Min K, Shindo K, Yan Y, Liao Y, Yamazaki S, Sanada S, Asano Y, Ishibashi-Ueda H, Takashima T, Minamino T, Asanuma H, Mochizuki N, Kitakaze M.
Dipeptidyl-Peptidase IV Inhibition Improves Pathophysiology of Heart Failure and Increases Survival Rate in Pressure-Overloaded Mice. Am J Physiol Heart Circ Physiol. 2013.

3) Yamazaki S, Kobayashi H, Takashima S, Liu W, Okuda H, Yan J, Fujii Y, Hitomi T, Harada KH, Habu T, Koizumi A.Ablation of Rnf213 retards progression of diabetes in the Akita mouse. Biochem Biophys Res Commun. 2013 Feb 11.

2、学会発表

1) 小林 果、山崎 悟、(5 人略).
ゼブラフィッシュモデルによるもやもや病感受性遺伝子 mysterin の機能解析 第 82 回日本衛生学会学術総会 2012 年 3 月

2) Daisuke Morito, (3人略)Satoru Yamazaki,(6人略).
Structure and Function of AAA+/ubiquitin ligase Mysterin/RNF213.FASEB summer research conferences " Quality Life through Research. Saxtons River 2012 年 7 月 USA

3) Yuri Kotani,(1人略), Satoru Yamazaki(4人略).
Regulation of mysterin, a moyamoya disease-associated protein, by de-ubiquitinating enzyme. EMBO/EMBL Symposium"Quality Control-From Molecules to Organelles-", Heiderberg 2012 年 9 月 Germany

4) Akira Funada (1 人略)Satoru Yamazaki,(10 人略).
Impact of the Polymorphisms of Renin-Angiotensin System on Prognosis in Hypertrophic Cardiomyopathy in the Era of Cardiac Magnetic Resonance 第 77 回日本循環器学会学術総会 2013 年 3 月

H. 知的財産権の出願・登録状況
(予定も含む)

1、特許取得
なし

2、実用新案登録
なし

3、その他
以上、特筆すべき事項なし

Cardiovasc Drugs Ther (2013) 27:125–132
DOI 10.1007/s10557-012-6437-6

ORIGINAL ARTICLE

Liposomal Amiodarone Augments Anti-arrhythmic Effects and Reduces Hemodynamic Adverse Effects in an Ischemia/Reperfusion Rat Model

Hiroyuki Takahama · Hirokazu Shigematsu · Tomohiro Asai · Takashi Matsuzaki · Shoji Sanada · Hai Ying Fu · Keiji Okuda · Masaki Yamato · Hiroshi Asanuma · Yoshihiro Asano · Masanori Asakura · Naoto Oku · Issei Komuro · Masafumi Kitakaze · Tetsuo Minamino

Published online: 24 January 2013

Abstract
Purpose Although amiodarone is recognized as the most effective anti-arrhythmic drug available, it has negative hemodynamic effects. Nano-sized liposomes can accumulate in and selectively deliver drugs to ischemic/reperfused (I/R) myocardium, which may augment drug effects and reduce side effects. We investigated the effects of liposomal amiodarone on lethal arrhythmias and hemodynamic parameters in an ischemia/reperfusion rat model.
Methods and Results We prepared liposomal amiodarone (mean diameter: 113±8 nm) by a thin-film method. The left coronary artery of experimental rats was occluded for 5 min followed by reperfusion. Ex vivo fluorescent imaging revealed that intravenously administered fluorescent-labeled nano-sized beads accumulated in the I/R myocardium. Amiodarone was measurable in samples from the I/R myocardium when liposomal amiodarone, but not amiodarone, was administered. Although the intravenous administration of amiodarone (3 mg/kg) or liposomal amiodarone (3 mg/kg) reduced heart rate and systolic blood pressure compared with saline, the decrease in heart rate or systolic blood pressure caused by liposomal amiodarone was smaller compared with a corresponding dose of free amiodarone. The intravenous administration of liposomal amiodarone (3 mg/kg), but not free amiodarone (3 mg/kg), 5 min before ischemia showed a significantly reduced duration of lethal arrhythmias (18±9 s) and mortality (0 %) during the reperfusion period compared with saline (195±42 s, 71 %, respectively).
Conclusions Targeting the delivery of liposomal amiodarone to ischemic/reperfused myocardium reduces the mortality due to lethal arrhythmia and the negative hemodynamic changes caused by amiodarone. Nano-size liposomes may be a promising drug delivery system for targeting I/R myocardium with cardioprotective agents.

Keywords Liposome · Amiodarone · Lethal arrhythmia · Ischemia · Reperfusion

T. Matsuzaki · S. Sanada · H. Y. Fu · K. Okuda · M. Yamato · Y. Asano · I. Komuro · T. Minamino (✉)
Department of Cardiovascular Medicine, Osaka University Graduate School of Medicine, 2-2 Yamadaoka, Suita, Osaka 565-0871, Japan
e-mail: minamino@cardiology.med.osaka-u.ac.jp

H. Takahama · M. Asakura · M. Kitakaze
Department of Cardiovascular Medicine, National Cerebral and Cardiovascular Center, Suita 565-8565, Japan

H. Shigematsu · T. Asai · N. Oku
Department of Medical Biochemistry and Global COE, University of Shizuoka Graduate School of Pharmaceutical Sciences, Shizuoka 422-8526 Shizuoka, Japan

H. Asanuma
Department of Cardiovascular Science and Technology, Kyoto Prefectural University School of Medicine, Kyoto 602-8566, Japan

H. Takahama
Division of Cardiovascular Disease, Mayo Clinic, Rochester, MN 55902, USA

Introduction

Therapies for the prevention and treatment of ischemia-induced life-threatening arrhythmias remain an unmet medical need [1]. Amiodarone is currently considered to be the most effective anti-arrhythmic drug available for treating life-threatening arrhythmias [2, 3], despite the fact that this compound has a negative impact on hemodynamic parameters [4, 5]. The intravenous administration of amiodarone is expected

to be beneficial for the immediate treatment of arrhythmias in emergency settings, such as acute myocardial infarction (AMI) [6, 7]. However, in clinical practice, the administration of amiodarone remains problematic for the treatment of AMI [8]. Although lower doses of amiodarone result in fewer incidences of death, high doses of amiodarone can cause hypotension and non-cardiac death, both of which may diminish the positive effects of amiodarone [8, 9]. Therefore, a novel delivery system is strongly desired to enhance the anti-arrhythmic effects of amiodarone without producing severe side effects.

Liposomes are widely used for drug delivery to actively or passively target specific organs and to improve drug stability in cancer and inflammatory diseases [10–12]. In ischemic/reperfused (I/R) myocardium, cellular permeability is enhanced and vascular endothelial integrity is disrupted [13, 14], suggesting that nanoparticles, such as liposomes, may be a promising drug delivery system for targeting I/R myocardium with cardioprotective agents [15]. Indeed, we have recently demonstrated that adenosine encapsulated by liposomes coated with polyethylene glycol (PEG) exhibited enhanced cardioprotective effects and attenuated side effects, such as hypotension and bradycardia, in an ischemia/reperfusion model of rats [16]. In the present study, we prepared liposomal amiodarone and examined 1) the targeted accumulation of liposomal amiodarone in the I/R myocardium, 2) the hemodynamic effects of the intravenous administration of liposomal amiodarone and free amiodarone, and 3) the anti-arrhythmic effects of these preparations in an I/R rat model. We showed that targeting the delivery of liposomal amiodarone to I/R myocardium reduces the mortality due to lethal arrhythmias and the negative hemodynamic changes caused by amiodarone in an I/R rat model.

Methods

Materials

The materials used to prepare PEGylated liposomes, including 1-palmitoyl-2-oleoyl-sn-glycero-3-phosphocholine (POPC), 1,2-dipalmitoyl-sn-glycero-3-phosphocholine (DPPC), cholesterol, and 1,2-distearoyl-sn-glycero-3-phosphoethanolamine-N-poly(ethylene glycol) 2000 (DSPE-PEG2000), were kindly donated by Nippon Fine Chemical Co. (Takasago, Hyogo, Japan). Fluorescent beads (diameter 100 nm) were purchased from Invitrogen. All other materials were obtained from Sigma-Aldrich (St. Louis, MO, USA).

Animals

Male Wistar rats (9 weeks old and weighing 250–310 g; Japan Animals, Osaka, Japan) were used. The animal experiments were approved by the Osaka University Research Committee and were performed according to institutional guidelines. All studies conformed to the Guide for the care and Use of Laboratory Animals published by the US National Institutes of Health (NIH Publication No. 85–23, revised 1996).

Preparation of PEGylated Liposomes

PEGylated liposomes composed of POPC, DPPC, cholesterol, DSPE-PEG2000, and amiodarone were prepared by a thin-film method. Briefly, amiodarone and lipids dissolved in chloroform were evaporated to form a thin lipid film using a rotary evaporator. The lipid film was dried for at least 1 h under reduced pressure and then hydrated with PBS (pH7.4). The liposome solution was freeze-thawed for 3 cycles with liquid nitrogen. The particle size of the liposomes was adjusted by extrusion through 100-nm-pore polycarbonate filters (Nuclepore, Cambridge, MA, USA). The liposomal solutions were centrifuged at 453,000 g for 15 min (CS120GXL, Hitachi, Japan) to remove the untrapped amiodarone. Then, the liposomes were resuspended in PBS. To determine the efficacy of trapping amiodarone in the liposomes, an aliquot of the liposomal solution was solubilized with 1 % reduced Triton X-100 (Sigma-Aldrich), and the amount of amiodarone was optically determined at 240 nm.

Characterization of PEGylated Liposomes

The particle size and ζ potential of PEGylated liposomes diluted with PBS were measured by dynamic scatter analysis (Zetasizer Nano ZS; Malvern, Worcestershire, UK). The analyses were performed 15 times per sample, and the results represent the analysis of 3 independent experiments.

Experimental Protocol

Targeted Delivery of Fluorescent-labeled Nano-sized Beads to the I/R Myocardium

The rats were anesthetized with intraperitoneal sodium pentobarbital (50 mg/kg). Catheters were advanced into the femoral vein to infuse the drugs. Ischemia/reperfusion was induced by 5 min of left coronary artery occlusion followed by reperfusion [16]. After the hemodynamic parameters became stable, fluorescent-labeled nano-size beads, 100 nm in diameter (FluoSpheres, Invitrogen), were intravenously infused to the rats for 5 min before ischemia or before a sham operation (n=3, each). Fifteen minutes after reperfusion, the hearts were removed and cut into 5 sections parallel to the axis from the base to the apex. Then, ex vivo fluorescence images were obtained with an Olympus SZX12 stereoscopic microscope equipped with a DP71 digital camera (Olympus, Tokyo, Japan) before and after the hearts were sliced.

Targeted Delivery of Amiodarone and Liposomal Amiodarone to the I/R Myocardium

Catheters were advanced into the femoral artery and vein to measure the systemic blood pressure (BP) and to infuse the drugs into the anesthetized rats, respectively. Electrocardiographic and hemodynamic parameters, such as heart rate (HR) and BP, were continuously monitored during the study using a PowerLab system (ADInstruments, Castle Hill, Australia). After the hemodynamic parameters became stable, to clarify the targeted delivery of amiodarone and liposomal amiodarone to the I/R myocardium, we intravenously administered saline, free amiodarone (3 mg/kg) or liposomal amiodarone (3 mg/kg) to rats for 5 min before the onset of ischemia. Then, we obtained blood samples and myocardium from the I/R area.

Effects of Amiodarone and Liposomal Amiodarone on Lethal Arrhythmias

To evaluate the effects of amiodarone and liposomal amiodarone on lethal arrhythmias, we intravenously administered saline (n=7), free amiodarone (3.0 or 10.0 mg/kg) (n=6 each), PEGylated liposomes (empty liposomes) (n=6), and PEGylated liposomal amiodarone (3.0 mg/kg) (n=6) for 5 min before ischemia. The dose of amiodarone used in this study was lower than that used in a previous study [17] to clarify whether amiodarone encapsulated by liposomes coated with PEG exhibited enhanced anti-arrhythmic effects. Without any procedure such as electrical conversion or cardiac massage, ventricular tachyarrhythmias (VT/VF) occurred frequently during early period of reperfusion and the mortality of rats reached more than a half of cases in this model [18].

Measurement of Amiodarone Concentration

The concentration of amiodarone in serum and heart tissue from the I/R area was assayed by high-performance liquid chromatography (HPLC) as previously described [19]. The detection limit of the HPLC assay was 50 ng/mL. Blood and myocardial samples were obtained at the end of the experimental protocol. The sample preparation was performed as previously described [19]. Briefly, myocardium was freed from visible blood, thereafter rinsed with 0.9 % sodium chloride and stored at −20 °C until analysis. After that, myocardial tissue samples were finely minced and 100 mg were homogenized with 0.9 % sodium chloride (1 mL) and after centrifugation, the clear supernatant was injected into HPLC.

Quantitative Evaluation of Fluorescent-labeled Nano-sized Beads in the I/R Myocardium

To analyze the quantitative fluorescent intensity, signals from heart slices were quantified by image analysis (Image J; National Institutes of Health, USA) as previously described [20]. The signal intensity from the heart slices was evaluated as the average signals of the whole heart and the left ventricle (LV) (Fig. 2c).

Arrhythmia Analysis

The electrocardiographic tracings were independently analyzed by two of the authors, who were blinded to the treatment assignment. The duration of each spontaneous ventricular tachycardia or fibrillation episode during the I/R protocol was measured using the time scale provided by the recording software. Ventricular tachycardia was defined as 4 or more consecutive ventricular ectopic beats, and ventricular fibrillation was defined as a signal in which the individual QRS deflections could not easily be distinguished from one another. However, distinguishing ventricular tachycardia from fibrillation was often difficult [21]; therefore, we report ventricular tachycardia and fibrillation collectively as ventricular tachyarrhythmias (VT/VF) in this study. VT/VF duration and mortality were evaluated for 5 min of ischemia followed by 15 min of reperfusion.

Statistical Analysis

The parameters of the liposomes are expressed as the mean ± standard deviation (SD). Other data are expressed as the average ± standard error of the mean (SEM). To compare the parameters of the liposomes, unpaired t-tests were performed. We performed the Welch t-test to compare the amiodarone concentration in the plasma and myocardium. For hemodynamic parameters, the data were assessed with the paired t-test for comparisons to the baseline within a group. One-way repeated-measurement ANOVA followed by post-hoc Bonferroni's multiple comparisons were used for comparisons between groups. To address the differences in VT/VF duration among the groups, we performed a non-parametric (Kruskal-Wallis) test followed by evaluation with the Mann–Whitney U test. The mortality rates were compared using the Fisher's exact probability test. In all analyses, P<0.05 was considered to be statistically significant.

Results

Characterization of PEGylated Liposomes

We prepared 5 types of PEGylated liposomes composed of POPC, DPPC, cholesterol, and amiodarone. The ratio of unsaturated lipids (POPC) to saturated lipids (DPPC) varied (Fig. 1). During preparation of the liposomes, the POPC:DPPC:cholesterol:amiodarone molar ratio of 10:0:5:1 exhibited the best encapsulation efficiency for amiodarone compared with the other conditions (Fig. 1).

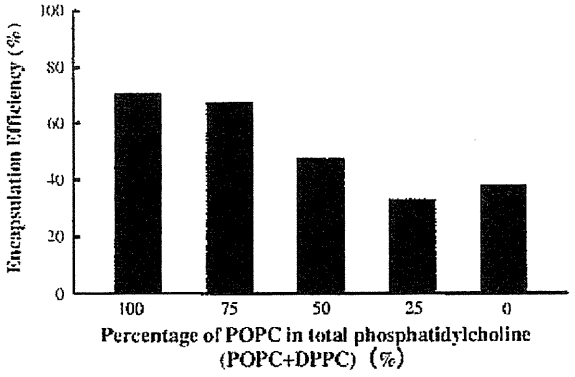

Fig. 1 Encapsulation efficiency of amiodarone in the liposomes. Amiodarone was loaded into liposomes containing POPC, DPPC, or a mixture of POPC and DPPC. The liposomal amiodarone was composed of phosphatidylcholine (POPC + DPPC):cholesterol:amiodarone at a 10:5:1 molar ratio. The percent molar ratio of POPC in total phosphatidylcholine (POPC + DPPC) is indicated in the figure. The encapsulation efficiency of amiodarone was determined as described in the Methods section

The dynamic light scatter analysis showed no significant differences between the mean diameter, polydispersity index, or ζ potential distribution of the empty and amiodarone-loaded PEGylated liposomes (Table 1).

Accumulation of Fluorescence-labeled Nano-sized Beads in the I/R Myocardium

Representative pictures obtained by fluorescence imaging are shown in Fig. 2a (whole heart) and b (sliced hearts). Quantitative analysis revealed that the average fluorescence intensity of the whole heart (Fig. 2c left) or the left ventricle (Fig. 2c right) of the I/R hearts was significantly higher than that in sham-operated hearts.

Amiodarone Concentration in the Blood and I/R Myocardium

The plasma concentration after the administration of liposomal amiodarone was significantly higher than that of free amiodarone (Table 2). Importantly, the amiodarone concentration in the I/R myocardium was detectable after the administration of liposomal, but not free, amiodarone (Table 2).

Hemodynamic Effects of Amiodarone and Liposomal Amiodarone

The baseline heart rates were 411±16, 426±14, 427±12, 409±8 and 414±6 beats/min in the saline, empty liposome, amiodarone (3 mg/kg), amiodarone (10 mg/kg) and liposomal amiodarone (3 mg/kg) groups, respectively. The baseline systolic BP was 113±7, 118±10, 111±5, 90±4 and 104±2 mmHg in the saline, empty liposome, amiodarone (3 mg/kg), amiodarone (10 mg/kg) and liposomal amiodarone (3 mg/kg) groups, respectively. There were no significant differences in the baseline HR or systolic BP among the groups tested. The intravenous administration of amiodarone (3 and 10 mg/kg) or liposomal amiodarone reduced both the HR and systolic BP from the baseline, whereas the saline or empty liposomes did not (Fig. 3). The time-course changes of both the HR and systolic BP were significantly smaller in the liposomal amiodarone group (3 mg/kg) compared with the corresponding dose in the free amiodarone group (3 mg/kg) (Fig. 3). The reductions in HR and systolic BP at 1, but not 3, minutes after liposomal amiodarone administration were significantly smaller compared with those following the corresponding dose of amiodarone.

Antiarrhythmic Effects of Amiodarone and Liposomal Amiodarone

Representative electrocardiograms of the rats that received saline, free amiodarone or liposomal amiodarone are shown in Fig. 4. The intravenous administration of liposomal amiodarone (3 mg/kg), but not amiodarone (3 mg/kg), significantly reduced the duration of VT/VF compared with saline (Table 3). Furthermore, the mortality in the group that received liposomal amiodarone (3 mg/kg), but not the corresponding dose of amiodarone (3 mg/kg), was significantly lower than that in the saline group. In the group of rats that received a high dose of amiodarone (10 mg/kg), the VT/VF duration was 36±12 s, and none of the rats died (Table 3), which was similar to the low dose of liposomal amiodarone group (3 mg/kg).

Discussion

In this study, we revealed that 1) liposomal amiodarone was successfully prepared using a thin-film method, 2) the

Table 1 Characterization of liposomes by dynamic light scatter analysis

	Mean diameter (nm)	Polydispersity index	ζ Potential (mV)
PEGylated liposomes (empty liposomes)	111±14	0.124±0.027	−2.1
PEGylated liposomal amiodarone	113±8	0.128±0.040	−3.7

Results represent 4 independent experiments. The values are expressed as the mean ± SD. *PEG* polyethylene glycol

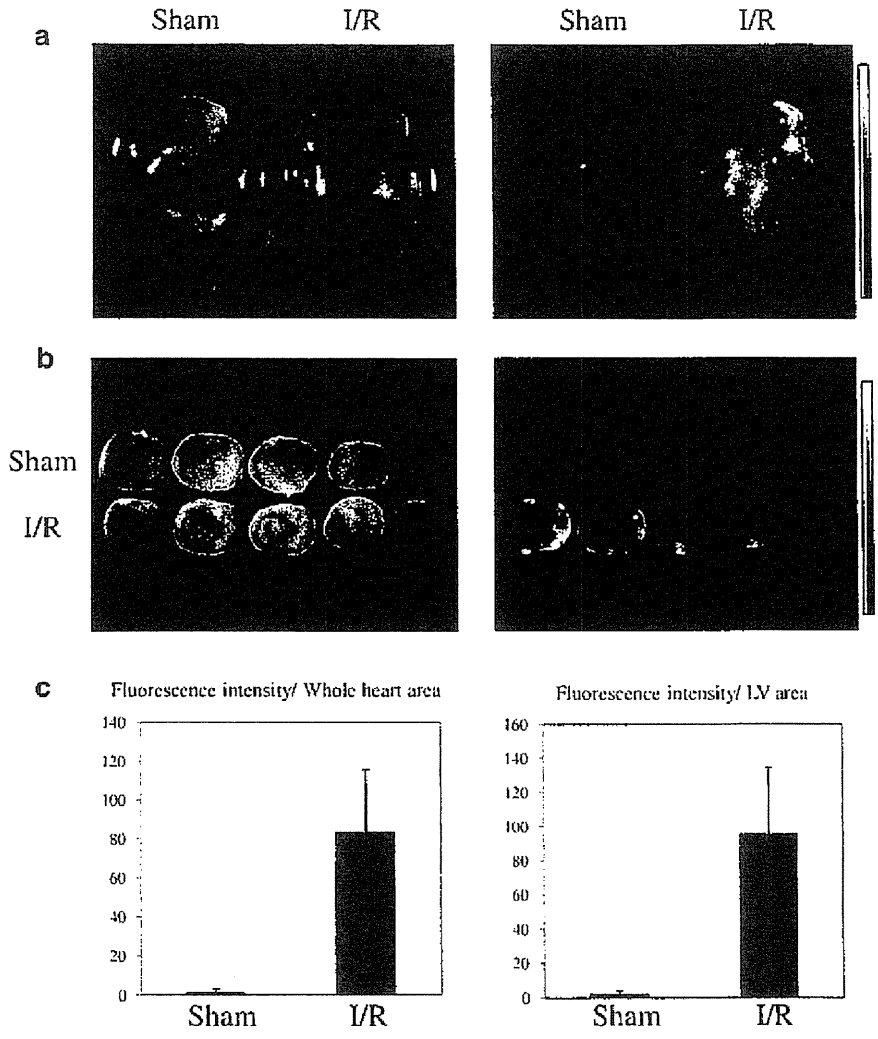

Fig. 2 Representative pictures of ischemia/reperfused myocardium with and without fluorescence-labeled nano-sized beads. Representative pictures obtained by fluorescent imaging are shown in **a** (*whole heart*) and **b** (*sliced hearts*). Quantitative analysis revealed that the average fluorescence intensity of the whole heart (**c** *left*) or the left ventricle (**c** *right*) of the I/R hearts was significantly higher than that of the sham-operated hearts

accumulation of nano-sized beads was observed in the I/R myocardium, 3) liposomal amiodarone showed a smaller reduction in the HR and systolic BP compared with free amiodarone, and 4) liposomal amiodarone, but not amiodarone, reduced the VT/VF duration and mortality during the reperfusion period compared with saline.

Table 2 Amiodarone concentration in the blood and I/R myocardium

Groups	Plasma, ng/mL	Myocardium, ng/mL
Saline	N.D.	N.D.
Free amiodarone	472±147	N.D.
Liposomal amiodarone	3872±378*	71±7*

Data are expressed as the mean ± SEM. *N.D.* not detected. $n=3$ rats in each group. * $p<0.05$ versus free amiodarone

Preparation of Liposomal Amiodarone

This study is the first to encapsulate amiodarone in PEGylated liposomes, although it has been previously encapsulated in other liposomes [22] and micelles [23]. We demonstrated that lipid bilayers composed of unsaturated lipids are more suitable for encapsulating amiodarone in PEGylated liposomes compared with those composed of saturated lipids. PEGylated liposomes have a long circulating time in the bloodstream because PEG endows a steric barrier to liposomes, allowing them to avoid interactions with opsonins and cells of the mononuclear phagocytic system [24]. Thus, they have been used to increase drug stability, safety, and bioavailability in clinical applications. In this study, we found that a higher concentration of amiodarone was retained in the blood when we administered liposomal amiodarone compared with the administration of

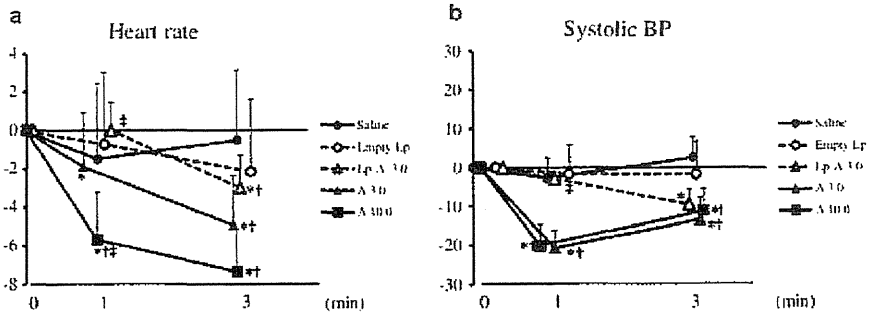

Fig. 3 Time-course changes in HR and systolic BP after drug administration. Shows the percent change from baseline for HR (a) and systolic BP (b) after intravenous administration of the tested drugs. The data are expressed as the mean ± SEM. *$P<0.05$ versus baseline, paired t-test. $P=0.0009$ (HR), 0.0002 (systolic BP) between amiodarone (3 mg/kg) and liposomal amiodarone (3 mg/kg). 1-way repeated-measurement ANOVA. †$P<0.05$ versus saline, ‡$P<0.05$ versus amiodarone (3 mg/kg), 1-way repeated-measurement ANOVA with Bonferroni's multiple comparison

free amiodarone, suggesting that encapsulation of amiodarone in PEGylated liposomes enhances the stability of amiodarone in the blood.

Targeted Delivery to the I/R Myocardium by Liposomal Amiodarone

Ex vivo fluorescence imaging revealed that fluorescence-labeled nano-sized beads accumulated in the I/R myocardium, suggesting that myocardial permeability can be enhanced in the I/R myocardium. Consistent with this finding, we observed that the amiodarone concentration in the I/R myocardium in the liposomal amiodarone group was much higher compared with that in the amiodarone group. Enhanced permeability in the I/R myocardium and the prolonged presence of amiodarone in PEGylated liposomes in the blood represent a possible mechanism for increased amiodarone concentrations in the I/R myocardium. Amiodarone will be released from accumulated liposomal amiodarone in I/R myocardium due to the natural decay and concentration gradient. These findings suggest that the I/R myocardium is a promising passive target for liposomal drug delivery.

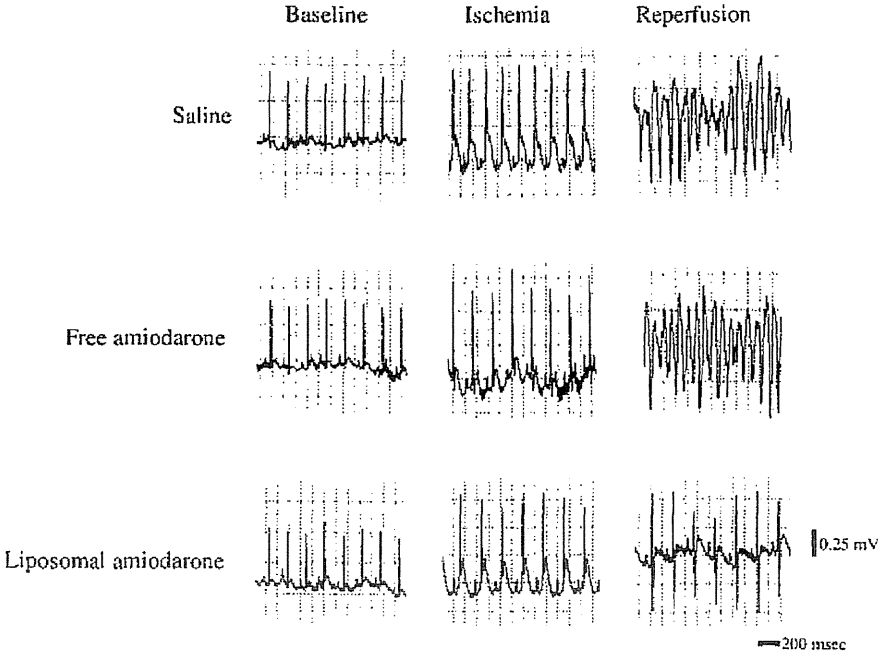

Fig. 4 Representative electrocardiograms. The *upper, middle and lower panels* show representative electrocardiograms under baseline conditions during ischemia and at the onset of reperfusion for rats that received saline, free amiodarone (3 mg/kg) and liposomal amiodarone (3 mg/kg), respectively

Table 3 Lethal arrhythmias and mortality in an I/R rat model

	Number	VT/VF duration (sec)	Mortality (%)
Saline	7	195±42	71
Empty liposomes	6	162±31	50
Amiodarone (3 mg/kg)	6	167±78	33
Amiodarone (10 mg/kg)	6	36±12*	0#
Liposomal Amiodarone (3 mg/kg)	6	18±9*	0#

*$p<0.05$ versus saline (VT/VF duration). #$p<0.05$ versus saline group (mortality). *VT* ventricular tachycardia. *VF* ventricular fibrillation

Minimal Negative Hemodynamic Effects of Liposomal Amiodarone

Amiodarone causes hypotension and bradycardia in clinical settings [4, 5]. In this study, both free and liposomal amiodarone significantly reduced the HR and systolic BP; however, the time-course changes for both the HR and systolic BP in the liposomal amiodarone group were significantly smaller compared with those following the corresponding dose of free amiodarone. Importantly, the reductions in HR and systolic BP at 1, but not 3, minutes after liposomal amiodarone administration were significantly smaller compared with those following the corresponding dose of amiodarone. These findings suggest that liposomal amiodarone may minimize the negative effects on systemic hemodynamics immediately after the administration of amiodarone. One possible mechanism to explain this finding is that amiodarone on the surface of the liposome membrane is covered with PEG so that amiodarone cannot act directly on cardiovascular cells. Gradual release of amiodarone from liposome may minimize the rapid hemodynamic changes, because systemic hemodynamic effects of liposomal amiodarone were significantly attenuated in liposomal amiodarone group than free amiodarone group.

Augmented Anti-arrhythmic Effects of Liposomal Amiodarone

In this study, liposomal amiodarone (3 mg/kg), but not the corresponding dose of free amiodarone (3 mg/kg), significantly reduced the VT/VF duration and mortality compared with saline in an I/R rat model. Because the acute effects of amiodarone are known to be attributable to blockade of Na^+, Ca^{2+} and dose-dependent K^+ channels [2, 25], increasing the concentration of amiodarone in the I/R myocardium may augment its anti-arrhythmic effects through its tonic effects on cardiomyocytes caused by blocking cardiac ionic currents. Kishida et al. reported that amiodarone enhances nitric oxide production in cultured human endothelial cells [26]. Furthermore, amiodarone protects cardiac myocytes against oxidative injury by scavenging free radicals [27]. These pleiotropic effects of amiodarone are also enhanced by its increased concentration in the I/R myocardium via PEGylated liposomes, which may contribute to the reduction of lethal arrhythmias during reperfusion followed by ischemia. In the present study, since we did not do any procedure such as electrical conversion or cardiac massage for VT/VF, the mortality was higher than in our previous report [16].

Clinical Implications

In clinical settings, higher doses of amiodarone cause hypotension and non-cardiac death or induce worsening heart failure through negative inotropic effects [28]. These effects often diminish the beneficial effects of amiodarone for patients with AMI or heart failure [8, 9]. The present study demonstrated that liposomal amiodarone (3 mg/kg) exerts anti-arrhythmic effects similar to a high dose of free amiodarone (10 mg/kg) while reducing the extent of bradycardia and hypotension, suggesting that encapsulating amiodarone in liposomes augments its anti-arrhythmic effects and reduces its negative effects on hemodynamic parameters with reducing administrative dose. These findings can have a great impact on preventing lethal arrhythmias during reperfusion in AMI patients.

Study Limitations

There are several limitations in this study. We used a brief period of I/R without myocardial infarction in rats. Sakamoto et al. demonstrated that the incidence of VT/VF in a rodent model was 'bell-shaped' with a maximum at 5 min of ischemia and that most lethal arrhythmias occurred within first 20 s after the onset of reperfusion [29]. Consistently, our data showed that the mean time at which the lethal arrhythmia occurred after the onset of reperfusion was 3.3+/−1.6 s. Therefore, we chose the 5 min of ischemia followed by 15 min of reperfusion model. We also chose the timing of drug administration before the onset of ischemia to clarify whether liposomal-amiodarone could prevent the lethal arrhythmia that occurs in the early period of reperfusion. In addition, in clinical practice lethal arrhythmias often occur after a brief period of I/R without any irreversible damage to the heart, indicating that the anti-arrhythmic effects of liposomal amiodarone during a brief period of ischemia model could have clinical relevance [30]. However, careful interpretation is necessary when using liposomal amiodarone in acute myocardial infarction with irreversible damage to confirm the beneficial effects of liposomal amiodarone. Furthermore, because the electrophysiology of rats differs from that of humans and drug administration in our study started before the onset of

ischemia, additional pre-clinical studies including a longer period of I/R model to consider the timing of drug administration are needed using large animal models. We should also take into account that the potential side effects of amiodarone such as bradycardia are minimal in the left coronary artery occlusion model used in the present study.

Conclusion

In conclusion, the targeted delivery of liposomal amiodarone to the I/R myocardium exerted strong anti-arrhythmic effects and reduced the negative impact on systemic hemodynamics. Nano-sized liposomes may be a promising drug delivery system for targeting the I/R myocardium with cardioprotective agents.

Acknowledgments The authors thank Takaki Hayakawa for her technical assistance, Takeshi Aiba for his special advice about data analysis. *This research was supported by Grants-in-Aid from the Ministry of Health, Labor, and Welfare of Japan; Grants-in-Aid from the Ministry of Education, Culture, Sports, Science, and Technology of Japan; grants from the Japan Heart Foundation; and grants from the Japan Cardiovascular Research Foundation.*

References

1. Di Diego JM, Antzelevitch C. Ischemic ventricular arrhythmias: experimental models and their clinical relevance. Hear Rhythm. 2011;8:1963–8.
2. Kodama I, Kamiya K, Toyama J. Cellular electropharmacology of amiodarone. Cardiovasc Res. 1997;35:13–29.
3. Vassallo P, Trohman RG. Prescribing amiodarone: an evidence-based review of clinical indications. JAMA. 2007;298:1312–22.
4. Scheinman MM, Levine JH, Cannom DS, et al. Dose-ranging study of intravenous amiodarone in patients life-threatening ventricular tachyarrhythmias. The Intravenous Amiodarone Multicenter Investigators Group. Circulation. 1995;92:3264–72.
5. Podrid PJ. Amiodarone: reevaluation of an old drug. Ann Intern Med. 1995;122:689–700.
6. Shiga T, Tanaka T, Irie S, Hagiwara N, Kasanuki H. Pharmacokinetics of intravenous amiodarone and its electrocardiographic effects on healthy Japanese subjects. Hear Vessel. 2011;26:274–81.
7. Wenzel V, Russo SG, Arntz HR, et al. [Comments on the 2010 guidelines on cardiopulmonary resuscitation of the European Resuscitation Council.]. Anaesthesist. 2010.
8. Elizari MV, Martinez JM, Belziti C, et al. Morbidity and mortality following early administration of amiodarone in acute myocardial infarction. GEMICA study investigators, GEMA Group, Buenos Aires, Argentina. Grupo de Estudios Multicentricos en Argentina. Eur Heart J. 2000;21:198–205.
9. Hu K, Gaudron P, Erl G. Effects of high- and low-dose amiodarone on mortality, left ventricular remodeling, and hemodynamics in rats with experimental myocardial infarction. J Cardiovasc Pharmacol. 2004;44:627–30.
10. Semalty A, Semalty M, Rawat BS, Singh D, Rawat MS. Pharmacosomes: the lipid-based new drug delivery system. Expert Opin Drug Deliv. 2009;6:599–612.
11. Whitehead KA, Langer R, Anderson DG. Knocking down barriers: advances in siRNA delivery. Nat Rev Drug Discov. 2009;8:129–38.
12. Malam Y, Loizidou M, Seifalian AM. Liposomes and nanoparticles: nanosized vehicles for drug delivery in cancer. Trends Pharmacol Sci. 2009;30:592–9.
13. Horwitz LD, Kaufman D, Keller MW, Kong Y. Time course of coronary endothelial healing after injury due to ischemia and reperfusion. Circulation. 1994;90:2439–47.
14. Dauber IM, VanBenthuysen KM, McMurtry IF, et al. Functional coronary microvascular injury evident as increased permeability due to brief ischemia and reperfusion. Circ Res. 1990;66:986–98.
15. Galagudza MM, Korolev DV, Sonin DL, et al. Targeted drug delivery into reversibly injured myocardium with silica nanoparticles: surface functionalization, natural biodistribution, and acute toxicity. Int J Nanomedicine. 2010;5:231–7.
16. Takahama H, Minamino T, Asanuma H, et al. Prolonged targeting of ischemic/reperfused myocardium by liposomal adenosine augments cardioprotection in rats. J Am Coll Cardiol. 2009;53:709–17.
17. Riva E, Hearse DJ. Anti-arrhythmic effects of amiodarone and desethylamiodarone on malignant ventricular arrhythmias arising as a consequence of ischaemia and reperfusion in the anaesthetised rat. Cardiovasc Res. 1989;23:331–9.
18. Canyon SJ, Dobson GP. Protection against ventricular arrhythmias and cardiac death using adenosine and lidocaine during regional ischemia in the in vivo rat. Am J Physiol Heart Circ Physiol. 2004;287:H1286–95.
19. Plomp TA, Wiersinga WM, Maes RA. Tissue distribution of amiodarone and desethylamiodarone in rats after repeated oral administration of various amiodarone dosages. Arzneimittelforschung. 1985;35:1805–10.
20. Feige JN, Sage D, Wahli W, Desvergne B, Gelman L. PixFRET, an ImageJ plug-in for FRET calculation that can accommodate variations in spectral bleed-throughs. Microsc Res Tech. 2005;68:51–8.
21. Opitz CF, Mitchell GF, Pfeffer MA, Pfeffer JM. Arrhythmias and death after coronary artery occlusion in the rat. Continuous telemetric ECG monitoring in conscious, untethered rats. Circulation. 1995;92:253–61.
22. Klibanov AL, Maruyama K, Torchilin VP, Huang L. Amphipathic polyethyleneglycols effectively prolong the circulation time of liposomes. FEBS Lett. 1990;268:235–7.
23. Theodossiou TA, Galanou MC, Palcos CM. Novel amiodarone-doxorubicin cocktail liposomes enhance doxorubicin retention and cytotoxicity in DU145 human prostate carcinoma cells. J Med Chem. 2008;51:6067–74.
24. Elhasi S, Astaneh R, Lavasanifar A. Solubilization of an amphiphilic drug by poly(ethylene oxide)-block-poly(ester) micelles. Eur J Pharm Biopharm. 2007;65:406–13.
25. Kamiya K, Nishiyama A, Yasui K, Hojo M, Sanguinetti MC, Kodama I. Short- and long-term effects of amiodarone on the two components of cardiac delayed rectifier K(+) current. Circulation. 2001;9:1317–24.
26. Kishida S, Nakajima T, Ma J, et al. Amiodarone and N-desethylamiodarone enhance endothelial nitric oxide production in human endothelial cells. Int Heart J. 2006;47:85–93.
27. Ide T, Tsutsui H, Kinugawa S, Utsumi H, Takeshita A. Amiodarone protects cardiac myocytes against oxidative injury by its free radical scavenging action. Circulation. 1999;100:690–2.
28. Freedman MD, Somberg JC. Pharmacology and pharmacokinetics of amiodarone. J Clin Pharamacol. 1991;31:1061–9.
29. Sakamoto J, Miura T, Tsuchida A, Fukuma T, Hasegawa T, Shimamoto K. Reperfusion arrhythmias in the murine heart: their characteristics and alteration after ischemic preconditioning. Basic Res Cardiol. 1999;94:489–95.
30. Tzivoni D, Keren A, Granot H, Gottlieb S, Benhorin J, Stern S. Ventricular fibrillation caused by myocardial reperfusion in Prinzmetal's angina. Am Heart J. 1983;105:323–5.

Circulation Journal
Official Journal of the Japanese Circulation Society
http://www.j-circ.or.jp

EDITORIAL

The Less Embraces the Greater in Detecting Multiple Coronary Artery Disease

Shoji Sanada, MD, PhD; Masafumi Kitakaze, MD, PhD; Issei Komuro, MD, PhD

Ischemic heart disease (IHD) is a major cause of mortality in both Western countries and Japan.[1] Recently, the morbidity and mortality of IHD have substantially improved because of progress in therapeutic strategies, represented by the dramatic evolution of percutaneous coronary intervention (PCI).[2] In fact, any sophisticated techniques in PCI are based on advanced imaging technologies to visualize the physical or structural causes of ischemia such as coronary stenosis or obstruction. However, as most cardiologists know, physical stenosis or obstruction does not necessarily reflect the incidence of myocardial ischemia in respective perfused regions within myocardium.[3]

Article p430

Myocardial ischemia ultimately originates from the mismatch in supply of energy substrates such as glucose, free fatty acids or oxygen in relation to myocardial energy demands within the cardiomyocytes;[4] however, in the majority of cases, it might be actually represented by a mismatch in local blood supply. Therefore, structural data on physical coronary stenosis or obstruction should be generally accompanied by information on regional "functional" shortage of blood supply to confirm regional myocardial ischemia. In that way, the somewhat conventional technology of single-photon emission computed tomography (SPECT), a semi-quantitative measurement of regional myocardial blood flow via blood flow-mediated myocardial incorporation of ions or metabolic substrates, is still widely accepted as a major and effective imaging strategy.[4] Primarily, it works best in detecting localized regional ischemia by prominently displaying low-flow areas in contrast with other good-flow areas by nature, and has some difficulty in precisely indicating multiple or global coronary ischemia.[5] One of the compensatory strategies for detecting such severe coronary artery disease (CAD) is to detect the stress-induced changes in dynamic cardiac performance, mainly by stress echocardiography.[6] Using this method, we can easily detect multiple or global coronary ischemia through a greater reduction in cardiac contractile performance upon stress.[7] ECG-based gated SPECT newly provides us with the additive information of dynamic changes in left ventricular chamber size and regional wall motion[5] that enable us to evaluate segmental blood flow and regional contractile function, namely physically and functionally active ischemia, at once and compare the integrated myocardial status with and without stress in a single modality.

Stress-induced ischemic changes in myocardial contractile performance mainly include transient postischemic myocardial stunning (PMS) and transient ischemic dilation (TID).[8] In this issue of the Journal, Hida et al[9] report on which phenomenon would better predict the existence of multiple coronary ischemia using 271 patients who underwent stress SPECT followed by coronary angiography (CAG). They found that PMS, defined as poststress increase in end-systolic volume (ESV) ≥5 ml, together with conventional criteria of multi-territorial ischemia in ATP-induced stress SPECT, best identified multiple CAD, with substantially high sensitivity (78%) and specificity (84%).

Intriguingly, although SPECT has been thought to be relatively weak in detecting broad ischemia, namely left main and/or 3-vessel disease,[5] the present study reports that this modality still tended to keep a satisfactory sensitivity of 74% and specificity of 57% with a poststress increase in ESV ≥5 ml, as well as those of 82% and 42%, respectively, with a poststress decrease in EF ≥2%, in detecting multiple coronary ischemia, whereas the TID ratio again turned out to be not significantly useful.[9] This finding has at least 2 notable aspects.

First, taken together with other sets of data that conventional diagnosis via multi-territorial malperfusion alone provides a similar sensitivity of 77%, but lower specificity of 55%, for predicting multiple coronary ischemia,[9] and that these values are not improved even in combination with an increased TID ratio,[9] the criteria proposed here (ie, PMS together with multi-territorial ischemia) has sufficient power of detecting broad and multiple CAD and might give substantial priority to stress SPECT test as a first-line extensive noninvasive examination following routine screening tests to diagnose multiple CAD in the clinical setting. In fact, invasive CAG is currently still serving as the best standard for detecting coronary structural stenosis because it can provide detailed and complicated information at once precisely, regardless of heart rate and arrhythmia. However, it is invasive and needs substantial X-ray exposure, as well as use of contrast medium. Recently, ECG-gated dynamic multidetector-row computed tomography has emerged as a possible alternative to CAG because of the striking progress in imaging and instrumental technology, but it also needs contrast medium, still has some restrictions in acquiring images against arrhythmia and tachycardia, and is

Received December 13, 2011; accepted December 13, 2011; released online December 23, 2011

Department of Cardiovascular Medicine, Osaka University Graduate School of Medicine, Suita (S.S., I.K.); Osaka University Health Care Center, Suita (S.S.); and Department of Clinical Research and Development (S.S., M.K.), Cardiovascular Medicine (M.K.), National Cerebral and Cardiovascular Center, Suita, Japan

Mailing address: Shoji Sanada, MD, PhD, Department of Cardiovascular Medicine, Osaka University Graduate School of Medicine, 2-2 Yamada-oka, Suita 565-0871, Japan. E-mail: s-sanada@cardiology.med.osaka-u.ac.jp

ISSN-1346-9843 doi:10.1253/circj.CJ-11-1456

weak in detecting accurate images around calcified regions, because of enhanced noise. Therefore, for patients with severe renal dysfunction or allergy to contrast medium who cannot choose these options, cardiac SPECT is one of a very few alternatives for the detection of myocardial functional ischemia, although it has another limitation of lacking images from the segments without live myocardium.

Second, this might give some clue to addressing the mechanistic consequences of ischemia-induced acute cardiac dysfunction. This study suggests that systolic dysfunction is more sensitive to ischemic stress than temporal dilation, implying that systolic dysfunction might be a primary reaction, leading to dilated changes and subsequent cardiac dysfunction.[8] This consequence is concomitant with the widely recognized idea from experimental animal studies,[10] also relevant in humans,[11] that myocardial stunning represented by immediate regional myocardial asystole is a primary reaction to acute ischemic stress, followed by cardiac bulging and dilation.[1] In that way, to detect regional reduced contraction immediately after acute ischemic stress might be quite a reasonable strategy of predicting multiple ischemic regions.

Although the accurate cutoff value should be further tested and adjusted in large-scale trials, this study potentiates the importance of gated SPECT as a quite helpful option for diagnosing multiple CAD in addition to contrast-based angiography. We hope that the present findings will help to diagnose and treat severe IHD more easily and feasibly, via an increased variety of modalities in real-world clinical medicine.

References

1. Sanada S, Komuro I, Kitakaze M. Pathophysiology of myocardial reperfusion injury: Preconditioning, postconditioning, and translational aspects of protective measures. *Am J Physiol Heart Circ Physiol* 2011; **301**: H1723–H1741.
2. Sanada S, Kitakaze M. Ischemic preconditioning: Emerging evidence, controversy and translational trials. *Int J Cardiol* 2004; **97**: 263–276.
3. Yanagisawa H, Chikamori T, Tanaka N, Hatano T, Morishima T, Hida S, et al. Correlation between thallium-201 myocardial perfusion defects and the functional severity of coronary artery stenosis as assessed by pressure-derived myocardial fractional flow reserve. *Circ J* 2002; **66**: 1105–1109.
4. Beller GA, Heede RC. SPECT imaging for detecting coronary artery disease and determining prognosis by noninvasive assessment of myocardial perfusion and myocardial viability. *J Cardiovasc Transl Res* 2011; **4**: 416–424.
5. Badheka AO, Hendel RC. Radionuclide cardiac stress testing. *Curr Opin Cardiol* 2011; **26**: 370–378.
6. Abdelmoneim SS, Dhoble A, Bernier M, Erwin PJ, Korosoglou G, Senior R, et al. Quantitative myocardial contrast echocardiography during pharmacological stress for diagnosis of coronary artery disease: A systematic review and meta-analysis of diagnostic accuracy studies. *Eur J Echocardiogr* 2009; **10**: 813–825.
7. Arruda-Olson AM, Juracan EM, Mahoney DW, McCully RB, Roger VL, Pellikka PA. Prognostic value of exercise echocardiography in 5,798 patients: Is there a gender difference? *J Am Coll Cardiol* 2002; **39**: 625–631.
8. Abidov A, Berman DS. Transient ischemic dilation associated with poststress myocardial stunning of the left ventricle in vasodilator stress myocardial perfusion SPECT: True marker of severe ischemia? *J Nucl Cardiol* 2005; **12**: 258–260.
9. Hida S, Chikamori T, Tanaka H, Igarashi Y, Shiba C, Hatano T, et al. Postischemic myocardial stunning is superior to transient ischemic dilation for detecting multivessel coronary artery disease. *Circ J* 2012; **76**: 430–438.
10. Bolli R. Mechanism of myocardial "stunning". *Circulation* 1990; **82**: 723–738.
11. Barnes E, Khan MA. Myocardial stunning in man. *Heart Fail Rev* 2003; **8**: 155–160.

Am J Physiol Heart Circ Physiol 304: H1361–H1369, 2013.
First published March 15, 2013; doi:10.1152/ajpheart.00454.2012.

Dipeptidyl-peptidase IV inhibition improves pathophysiology of heart failure and increases survival rate in pressure-overloaded mice

Ayako Takahashi,[1,4] Masanori Asakura,[2] Shin Ito,[1] Kyung-Duk Min,[1] Kazuhiro Shindo,[1,4] Yi Yan,[4] Yulin Liao,[6] Satoru Yamazaki,[1] Shoji Sanada,[5] Yoshihiro Asano,[4,5] Hatsue Ishibashi-Ueda,[3] Seiji Takashima,[4,5] Tetsuo Minamino,[5] Hiroshi Asanuma,[7] Naoki Mochizuki,[1] and Masafumi Kitakaze[2]

[1]Department of Cell Biology, [2]Department of Clinical Research and Development, and [3]Division of Pathology, National Cerebral and Cardiovascular Center, Osaka, Japan; [4]Department of Molecular Cardiology and [5]Department of Cardiovascular Medicine, Osaka University Graduate School of Medicine, Osaka, Japan; [6]Department of Cardiology, Nanfang Hospital, Southern Medical University, Guangzhou, China; and [7]Department of Cardiology, Kyoto Prefectural University School of Medicine, Kyoto, Japan

Submitted 12 June 2012; accepted in final form 25 January 2013

Takahashi A, Asakura M, Ito S, Min KD, Shindo K, Yan Y, Liao Y, Yamazaki S, Sanada S, Asano Y, Ishibashi-Ueda H, Takashima S, Minamino T, Asanuma H, Mochizuki N, Kitakaze M. Dipeptidyl-peptidase IV inhibition improves pathophysiology of heart failure and increases survival rate in pressure-overloaded mice. *Am J Physiol Heart Circ Physiol* 304: H1361–H1369, 2013. First published March 15, 2013; doi:10.1152/ajpheart.00454.2012.—Incretin hormones, including glucagon-like peptide-1 (GLP-1), a target for diabetes mellitus (DM) treatment, are associated with cardioprotection. As dipeptidyl-peptidase IV (DPP-IV) inhibition increases plasma GLP-1 levels in vivo, we investigated the cardioprotective effects of the DPP-IV inhibitor vildagliptin in a murine heart failure (HF) model. We induced transverse aortic constriction (TAC) in C57BL/6J mice, simulating pressure-overloaded cardiac hypertrophy and HF. TAC or sham-operated mice were treated with or without vildagliptin. An intraperitoneal glucose tolerance test revealed that blood glucose levels were higher in the TAC than in sham-operated mice, and these levels improved with vildagliptin administration in both groups. Vildagliptin increased plasma GLP-1 levels in the TAC mice and ameliorated TAC-induced left ventricular enlargement and dysfunction. Vildagliptin palliated both myocardial apoptosis and fibrosis in TAC mice, demonstrated by histological, gene and protein expression analyses, and improved survival rate on *day 28* (TAC with vildagliptin, 67.5%; TAC without vildagliptin, 41.5%; $P < 0.05$). Vildagliptin improved cardiac dysfunction and overall survival in the TAC mice, both by improving impaired glucose tolerance and by increasing GLP-1 levels. DPP-IV inhibitors represent a candidate treatment for HF patients with or without DM.

heart failure; impaired glucose tolerance; dipeptidyl-peptidase IV inhibitor

HEART FAILURE (HF) is a leading causes of death in humans worldwide (1, 20, 37, 56), and is often linked to impaired glucose tolerance or diabetes mellitus (DM) (21, 53). DM is a major risk factor for cardiac dysfunction; Lind et al. (28) reported that poor glycemic control among patients with type 1 DM led to a high incidence of cardiovascular events. The energetic substrate utilization of cardiomyocytes under hyperglycemic conditions shifts from glucose to fatty acid oxidation, leading to HF (38). In DM, oxidative stress also causes endothelial dysfunction and decreases endothelial NO release, inducing microangiopathy (13, 31). Either glucose abnormalities or diabetes commonly exists in patients with HF, but as previously reported, patients with diabetes have no worse outcome of HF (50). Our previous clinical study revealed that ~90% of patients with chronic HF had impaired glucose tolerance (21).

Incretin hormones have recently been proposed as new targets for DM treatment. Glucagon-like peptide-1 (GLP-1) is an incretin hormone secreted from the lower intestines and colon, which stimulates insulin secretion from pancreatic beta cells. Its receptors are ubiquitously expressed, including in the cardiovascular system (8). GLP-1 is thought to possess cardioprotective properties because of the following three reasons: *1*) GLP-1 receptors localize to cardiomyocytes and endothelial cells (3, 57); *2*) activation of GLP-1 receptors increases phosphoinositide 3 (PI3)-kinase, serine/threonine protein kinase Akt (Akt), and extracellular signal-regulated kinase phosphorylation, potentially mediating cardioprotection (6, 19); and *3*) activation of GLP-1 receptors stimulates p38 mitogen-activated protein (MAP) kinase and endothelial nitric oxide synthase via protein kinase A activation, putatively affecting cardioprotection (5, 59) and plasma glucose normalization (16). As dipeptidyl-peptidase IV (DPP-IV) rapidly degrades GLP-1, which has a biological half-life of approximately 1.5–5 min (11, 18), both GLP-1 analogs and DPP-IV inhibitors have been developed as new drugs to treat type 2 DM. GLP-1 analogs reportedly ameliorate not only DM but also HF and myocardial ischemia (15, 33, 34, 48, 59), suggesting that DPP-IV inhibitors function cardioprotectively. Indeed, DPP-IV inhibitors are reportedly effective against myocardial infarction in mice and pacing-induced heart failure in pigs (14, 42, 59), suggesting that DPP-IV inhibitors may also affect the survival rate. However, the effects of DPP-IV inhibitors on the pathophysiology of pressure-overloaded HF and survival after HF are unknown.

We aimed to clarify whether vildagliptin, a DPP-IV inhibitor, improves the pathophysiology of HF and increases survival rate in pressure-overloaded mice.

METHODS

All of the animal care procedures were performed according to the American Physiological Society "Guiding Principles in the Care and Use of Vertebrate Animals in Research and Training" and with the approval of the ethical committee of Osaka University.

Address for reprint requests and other correspondence: M. Asakura, Dept. of Clinical Research and Development, National Cerebral and Cardiovascular Center, 5-7-1, Fujishirodai, Suita, Osaka, 565-8565 Japan (e-mail: masakura@ncvc.go.jp).

Animal preparation. Male C57BL/6J mice (8 wk old, weighing 22–24 g) were purchased from CLEA Japan, (Tokyo, Japan). After 1 wk of observation, either transverse aortic constriction (TAC) or a sham operation was performed as previously described (24). In brief, the transverse aorta was isolated between the carotid arteries and constricted by a 7-0 silk suture ligature tied firmly against a 30-gauge needle. Sham-operated mice underwent a similar surgical procedure without aortic constriction. The needle was promptly removed, and the chest was closed with a 5-0 silk suture. Each surgical procedure was completed within 30 min to maintain the body temperature at 37°C.

Experimental protocol. Vildagliptin was gifted by Novartis Pharmaceuticals (Basel, Switzerland). The sham-operated or TAC mice were randomly divided into two subgroups; the sham-operated group with (n = 10) or without vildagliptin (n = 10) and TAC with (n = 40) or without vildagliptin (n = 41). The vildagliptin treatment subgroups were provided with drinking water containing vildagliptin (10 mg·kg body wt^{-1}·day^{-1}) (39, 58), and the other groups received unsupplemented drinking water from 1 day postsurgery. The mice were allowed to drink ad libitum, and the drinking volumes were measured. The mice were fed a normal chow diet for 4 wk.

Echocardiography. Transthoracic echocardiography was performed before euthanasia as previously described (24). In brief, at 4 wk postsurgery, the mice were placed in a supine position without anesthesia. Short-axis, two-dimensional guided M-mode Doppler echocardiograms were captured and analyzed offline using a Vevo 770 High-Resolution in vivo Micro-Imaging System (VisualSonics, Toronto, Canada) equipped with a 15- to 45-MHz transducer. Left ventricular (LV) end-diastolic diameter (Dd), end-systolic diameter (Ds), and fractional shortening (FS) were measured. All measurements were made from leading edge to leading edge, according to the American Society of Echocardiography guidelines (22). Percentage FS was calculated as follows: %FS = [(LVDd − LVDs)/LVDd] × 100. The investigator performing and interpreting the echocardiograms was blinded to the subgroups.

Hemodynamic assessment. To confirm pressure overload, four to five mice in each group were randomly selected for LV pressure measurement, as previously described (27). In brief, under pentobarbital anesthesia, an endotracheal tube was inserted and connected to a volume-cycled rodent ventilator. A 1.4-Fr micromanometer-tipped catheter (Millar Instruments, Houston, TX) was inserted into the right carotid artery, blood pressure and heart rate were measured simultaneously, and data were acquired using the PowerLab Data Acquisition System (AD Instruments, Bella Vista, NSW, Australia).

Analysis of intraperitoneal glucose tolerance test. Four weeks after either TAC or sham operation, about half of the surviving mice, namely five mice in each sham-operated group and 12 and 8 mice in TAC with and without vildagliptin groups, were randomly selected for an intraperitoneal glucose tolerance test following overnight fasting (12–16 h). As overnight fasting and glucose injection might be stressful, we enrolled only half of the surviving mice to reduce the effect on additional deaths. Glucose (1 mg/kg body wt) was injected into the intraperitoneal cavity, as previously described (54). Blood was sampled from the tail prior to and at 30, 60, 90, and 120 min after glucose administration. Blood glucose concentrations were measured by a glucose meter using the glucose oxidase method (Glutest Ace R; Sanwa Kagaku Kenkyusho, Nagoya, Japan).

GLP-1 measurement [ELISA]. Four weeks after treatment, their chests were opened under anesthesia 1 h after feeding following overnight fasting for GLP-1 measurement by enzyme-linked immunosorbent assay (ELISA). Blood samples were obtained from the hearts and immediately collected in BD P700 tubes (Becton Dickinson, Franklin Lakes, NJ) containing EDTA and DPP-IV protease inhibitor cocktail. The tubes were centrifuged at 1,200 g for 10 min to extract plasma. The plasma samples were then stored at −80°C in a freezer until GLP-1 assay. Plasma GLP-1 levels were measured using a Glucagon-Like Peptide-1 (Active) ELISA Kit (Millipore, Billerica, MA) according to the manufacturer's instructions (52). The GLP-1 ELISA measures biologically active GLP-1-(7–37) and GLP-1-(7–36)-NH_2 but does not cross-react with glucagon, GLP-2, inactive GLP-1-(9–37) or GLP-1-(9–37)-NH_2.

Histology and immunohistochemistry. Histochemical analysis was performed as previously described (25). Briefly, the surviving mice were euthanized after 4 wk of observation. The hearts were harvested, and cardiac tissues were fixed with 4% paraformaldehyde. The fixed samples were embedded in paraffin and sectioned at 4-μm thickness for picrosirius red staining. The extent of myocardial collagen was analyzed in five hearts from each group (30). The original images were digitized and transformed into binary images, and each area was calculated using ImageJ software (NIH, Bethesda, MD). The total myocardial collagen index was defined as the total area of collagen content in the entire microscopic field divided by the total connective tissue area plus the myocardial area. The terminal deoxynucleotidyl transferase dUTP nick-end labeling (TUNEL) assay was performed using an ApopTag Peroxidase In Situ Apoptosis Detection Kit (Millipore), according to the manufacturer's instructions. The number of TUNEL-positive cells was expressed as a percentage of total cells, as previously described (35).

Real-time quantitative polymerase chain reaction. Four weeks after TAC, murine ventricles were processed for total RNA isolation using TRIzol reagent (Invitrogen, Carlsbad, CA) according to the manufacturer's instructions. First-strand cDNA was synthesized from 1 μg total RNA using the High-Capacity cDNA Reverse Transcription Kit (Applied Biosystems, Foster City, CA). The primers and probes used to quantify *transforming growth factor-1β (Tgf-1β)* and *glyceraldehyde 3-phosphate dehydrogenase (Gapdh)* were recommended by the manufacturer (Applied Biosystems). Real-time quantitative reverse transcriptase polymerase chain reaction (RT-PCR) was performed in a StepOne Real-Time PCR System (Applied Biosystems). From each amplification plot, a threshold cycle (Ct) value was calculated, representing the PCR cycle number at which fluorescence was detectable above an arbitrary threshold. Each sample was analyzed in duplicate, and the results were systematically normalized to GAPDH expression using the ΔΔCt method (29).

Western blot analysis. LV samples frozen at −80°C were placed on ice, homogenized, and lysed with lysis buffer [1% NP-40, 150 mM NaCl, 20 mM Tris pH 7.5, 2 mM EDTA, 50 mM NaF, 1 mM Na_3VO_4, plus protease inhibitor cocktail (Nacalai tesque, Kyoto, Japan)]. The supernatant was loaded onto 10%–15% sodium dodecyl sulfate-polyacrylamide gel electrophoresis gels. Immunoblotting was performed as previously described (41). The ChemiDoc XRS System (Bio-Rad Laboratories, Hercules, CA) was used for chemiluminescence imaging. Primary antibodies against phospho-Smad2 (p-Smad2), p-Smad3, caspase-3, and cleaved caspase-3 primary antibodies were purchased from Cell Signaling Technology (Beverly, MA); anti-Smad2/3 primary antibody was purchased from BD Transduction Laboratories (Franklin Lakes, NJ); and anti-GAPDH (used as a loading control) primary antibody was purchased from Millipore. Target bands were identified using ECL prime and ECL Select Western blotting reagents (GE Healthcare, Little Chalfont, Buckinghamshire, UK). Protein bands were quantified by densitometry.

Statistical analysis. All of the data are expressed as means ± SE and were analyzed by repeated-measures analysis of variance (ANOVA) followed by Bonferroni test and Student's t-test for paired and nonpaired data as appropriate. The differences in the number of surviving mice were analyzed by Kaplan-Meier method. P values of <0.05 were considered significant using JMP 8.0.1 software (SAS Institute, Cary, NC).

RESULTS

Hemodynamic measurements. The blood pressures and heart rates 4 wk after TAC were similar in the sham-operated groups with and without vildagliptin (71.2 ± 3.1 vs. 74.5 ± 3.2

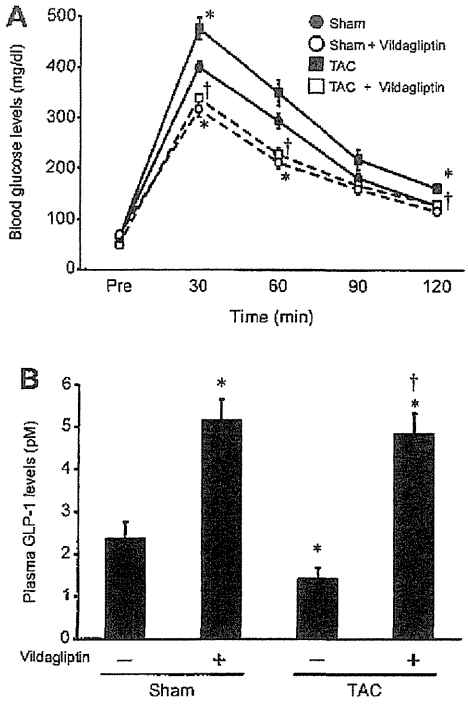

Fig. 1. *A*: plasma glucose levels measured by intraperitoneal glucose tolerance test. Sham-operated mice (n = 5), sham-operated mice with vildagliptin (n = 5), mice with transverse aortic constriction (TAC) (n = 8), and TAC mice with vildagliptin (n = 12) were enrolled. *B*: plasma levels of glucagon-like peptide-1 (GLP-1) 4 wk after TAC or sham operation. All blood samples were collected 1 h after feeding following overnight fasting. Sham-operated (n = 8), sham-operated mice with vildagliptin (n = 10), TAC mice (n = 15), and TAC mice with vildagliptin (n = 21) were measured. The data shown are means ± SE. *P < 0.05 vs. sham operated, †P < 0.05 vs. TAC.

mmHg; 459 ± 36 vs. 451 ± 22 beats/min; P = 0.482 and P = 0.830, respectively; n = 5 in each group), and in the TAC groups with and without vildagliptin (101.4 ± 9 vs. 121.4 ± 10 mmHg; 394 ± 80 vs. 463 ± 27 beats/min; P = 0.193 and P = 0.400; n = 5 and n = 4, respectively).

Intraperitoneal glucose tolerance test and plasma GLP-1 levels. Figure 1*A* shows the results of the intraperitoneal glucose tolerance test. Blood glucose levels at 30 and 120 min after intraperitoneal glucose injections were higher in the TAC mice than in the sham-operated mice (TAC vs. sham operated: 476.4 ± 20.9 vs. 400.5 ± 11.2 mg/dl at 30 min, and 161.5 ± 9.4 vs. 127.3 ± 8.3 mg/dl at 120 min, n = 8 and 5; P < 0.05). This was consistent with our previous report (27) in which TAC mice exhibited impaired glucose tolerance. Vildagliptin administration decreased blood glucose levels at each time point after glucose injection in TAC mice (with vs. without vildagliptin: 345.1 ± 7.9 vs. 476.4 ± 20.9 mg/dl at 30 min, 245.5 ± 13.1 vs. 349.6 ± 25.3 mg/dl at 60 min, and 127.9 ± 8.5 vs. 161.5 ± 9.4 mg/dl at 120 min, n = 12 and 8; P < 0.05).

We evaluated the GLP-1 levels in the TAC mice with or without vildagliptin. Because ad libitum feeding could have affected the plasma GLP-1 levels, we conducted a preliminary experiment to identify the optimal conditions for GLP-1 measurement. Nine-week-old C57BL6/J mice were fed a normal chow diet, divided into two groups, and treated with or without vildagliptin for 4 wk, as described above. To evaluate whether feeding affected the plasma GLP-1 levels, the mice were fasted 12 h before blood sampling. We randomly separated each group into two subgroups; the two subgroups were fasted further, and the others were allowed to feed 1 h before sampling. Under fasting conditions, vildagliptin produced a statistically insignificant increase in GLP-1 levels (with vs. without vildagliptin: 5.19 ± 1.04 vs. 3.93 ± 0.70 pM, n = 5 each; P > 0.05). In the mice sampled 1 h after feeding, GLP-1 levels were elevated with in the vildagliptin group (with vs. without vildagliptin: 9.13 ± 2.35 vs. 4.47 ± 0.87 pM, n = 4 and 5; P < 0.05), suggesting that this sampling time schedule, i.e., 1 h after food intake, was suitable for plasma GLP-1 measurement. Figure 1*B* shows the plasma GLP-1 levels under this time schedule. The GLP-1 levels were decreased in the TAC mice (sham operated vs. TAC: 2.37 ± 0.40 vs. 1.41 ± 0.26 pM, n = 8 and 15; P < 0.05), but elevated in TAC mice with vildagliptin to the levels of sham-operated mice with vildagliptin (with vs. without vildagliptin: 4.83 ± 0.50 vs. 1.41 ± 0.26 pM, n = 21 and 15; P < 0.05).

Echocardiography. Representative echocardiographic images are shown in Fig. 2. Echocardiographic analysis revealed enlarged Dd and Ds in the TAC mice both with and without vildagliptin (n = 27 and 17). Both LV dilatation and dysfunction in the TAC group were ameliorated by vildagliptin treatment (Fig. 3).

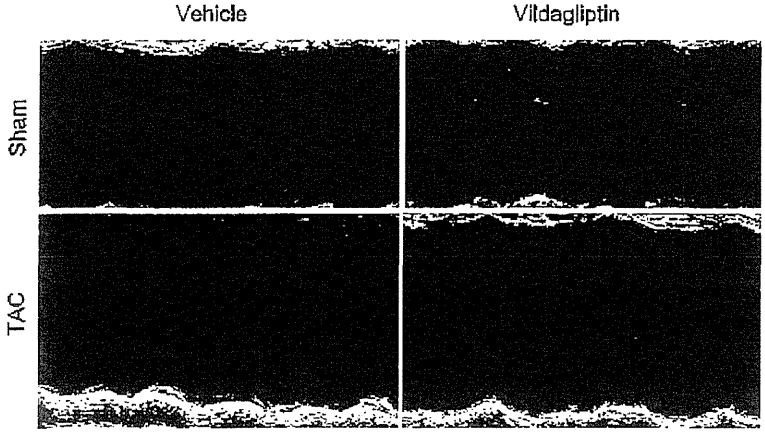

Fig. 2. Representative M-mode echocardiograms of mice 4 wk after TAC or sham operation. Top left, sham operated; top right, sham operated with vildagliptin; bottom left, TAC; bottom right, TAC with vildagliptin.